Supporting Information

Antimicrobial Silver Targets Glyceraldehyde-3-phosphate Dehydrogenase in Glycolysis of E. coli

Haibo Wang[a], Minji Wang[b], Xinming Yang[a], Xiaohan Xu[a], Quan Hao[c], Aixin Yan[b], Menglong Hu[c], Ryszard Lobinski[d], Hongyan Li[a]& Hongzhe Sun[a*]

[a]*Department of Chemistry, The University of Hong Kong, Hong Kong, P. R. China. E-mail: hsun@hku.hk*

[b]*School of Biological Sciences, The University of Hong Kong, Hong Kong, P. R. China.*

[c]*School of Biomedical Sciences, The University of Hong Kong, Laboratory Block, 21 Sassoon Road, Pokfulam, Hong Kong, China.*

[d]*Université de Pau et des Pays de l'Adour/CNRS, Laboratoire de Chimie Analytique Bio-inorganique et Environnement, IPREM-UMR5254, Hélioparc, 2, Avenue Angot, 64053, Pau, France.*

Table of Contents

Table of Contents **2**

Experimental Procedures **4**

Materials and experimental design 4

Materials 4

Standard protein iodination. 4

Bacterial culture and protein extraction. 4

Silver-binding protein separation and identification 4

DNA manipulation and plasmid construction 5

Protein expression and purification 5

GE-ICP-MS of purified proteins 6

Cellular thermal shift assay (CETSA) 6

In vivo enzymatic activity measurement 6

Mass spectrometry of purified proteins 7

Silver content determination in GAPDH and mutant proteins 7

Ellman assay 7

Isothermal titration calorimetry 7

Enzyme inhibition assay 7

Michaelis-Menten kinetics 8

X-ray crystallography 8

Effect of Ag^+ on *E. coli* growth 8

Statistical analysis 9

Supplementary Figures **10**

Figure S1. Overexpression and purification of GAPDH and IDH 10

Figure S2. Ag^+ binding to GAPDH mutants monitored by Ellman's assay. 11

Figure S3. Mass spectra of $GAPDH^{3CS}$ with or without incubation of Ag^+ 12

Figure S4. Isothermal titration calorimetry (ITC) results of Ag^+ binding to GAPDH mutants $GAPDH^{C149S}$, $GAPDH^{C153S}$ and $GAPDH^{C288S}$.. 13

Figure S5. Crystal and structure of apo and Ag-bound GAPDH.. 14

Figure S6. The effect of site-directed mutation of His176 to Ser on the function of GAPDH. 15

Figure S7. The effect of site-directed mutation of Cys153 and Cys288 to Ser on the function of GAPDH. 17

Figure S8. Bacterial growth and IC50 test. 17

Supplementary Tables **18**

Table S1. Summary of standard proteins used for iodine labelling in this study. 18

Table S2. Summary of identified Ag^+-binding proteins in *E. coli*. 19

Table S3. Strains, plasmids for protein expression. 20

Table S4. Primers for plasmid construction 21

Table S5. Summary of isothermal titration calorimetry data. 22
Table S6. Enzyme kinetics of GAPDH with or without treatment of Ag^{+}. 23
Table S7. Summary of X-ray crystallographic data collection and refinement statistics. 24

Experimental Procedures

Materials and experimental design

Materials

E. coli K12 MG 1655 is from our lab collection. The FPLC system was purchased from GE Healthcare. The column gel electrophoresis separation system was modified from a commercially available Mini Prep Cell system (Bio-Rad), using the newly designed gel column (Φ = 2.5 mm) and replacing the solution-transferring tubing (Φ = 0.25 mm PEEK tubing). Inductively coupled plasma mass spectrometry (ICP-MS) detections were performed on the Agilent 7700× system. Peptide mass fingerprinting was performed on an LTQ Orbitrap VelosTM mass spectrometer (Thermo Fisher Scientific). Unless otherwise specified, all chemical reagents and standard proteins were purchased from Sigma-Aldrich. The GAPDH activity assay kit (ab204732) and anti-GAPDH antibody (ab181602) were purchased from Abcam. All solutions were prepared from Milli-Q water (Milli-Q Ultrapure water systems, Millipore).

Standard protein iodination.

The iodination of standard proteins for internal calibration were carried out according to a previous report.[1] Briefly, potassium iodide (KI_3) solution of 50 mM is saturated with elemental iodine and used for the iodination reaction. The protein solution in the concentration of 1 mg/ml was incubated with KI_3 with a concentration of 5 mM for 10 mins at room temperature. Sodium dithionite was added to stop the reaction. The free iodide in proteins solution was removed by washing with PBS for three times. GE-ICP-MS was used to confirm the iodination of the proteins. One dimensional slab gel electrophoresis was applied to calibrate the molecular masses of iodinated proteins to avoid the apparent mass shift caused by any modification.

Bacterial culture and protein extraction.

E. coli cells from frozen stock were inoculated on Luria-Bertani (LB) agar plate and cultured at 37 °C overnight. Single colonies were grown in LB broth for overnight at 37 °C. Cells were then diluted by 1:100 to LB media and grown for *ca.* 2~3 hrs to the OD_{600} of 0.3. $AgNO_3$ at the concentration of 24 μM were then added into culture. Cells after treatment of $AgNO_3$ were harvested by centrifugation (4, 500 × g, 15 mins at 4 °C) and washed with cold phosphate-buffered saline (PBS) for 3 times. Collected pellets were resuspended in PBS buffer and then lysed through sonication (amplitude: 20%, 5 secs on, 20 secs off, in total 5 mins on the ice-water bath). The mixed suspension after sonication was centrifuged to get the supernatant. The supernatant was further centrifuged (10 mins, 100, 000 × g and 4 °C), fractionated, and subjected to GE-ICP-MS study after measuring the protein concentration by Pierce™ BCA Protein Assay Kit (Thermo Fisher Scientific).

Silver-binding protein separation and identification.

The GE-ICP-MS experiment was performed according to our previous study.[2] In brief, a reverse multilayer native resolving gel (13%→10% with lengths of 1.4 and 2.0 cm respectively) and 4% stacking gel of 0.6 cm were utilized to resolve proteins. A two-step procedure with 200 V (40 mins) for protein stacking and 600 V for resolving was applied. At the beginning of the second step, ICP-MS detection was started for elemental detection. The conditions for GE-ICP-MS were kept the same for all experiments. ^{127}I-labelled proteins were added as internal standards for MW calibration. I-CA was selected for the calibration

of intensity of silver-binding proteins. To split the protein solutions after column gel electrophoresis, a T-connection connected with additional pump tubing with same diameter was employed to transfer half of the eluted solutions to an automatic sample collection system. 100 µl eluents were collected in each tube. One-dimensional slab gel electrophoresis was applied to separate the collected fractions after reducing sample volume with ultrafiltration device with molecular weight cut-off of 3 kDa. Verified single band in the one-dimensional SDS PAGE gel was cut for MS identification.

The proteins in gel pieces were extracted and identified through peptide mass fingerprinting according to the standard protocol. In general, the proteins in gel pieces were extracted twice using 5% formic acid (FA)/50% acetonitrile (ACN) and then extracted once with 100% ACN. After purification by Ziptip (Millipore), the desalted peptides were mixed in a 1:1 ratio with 10 mg/ml α-cyano-4-hydroxycinnamic acid matrix (Fluka) dissolved in 0.1% FA/50% ACN.

The samples were injected via a nanospray chamber equipped with a gold coated nanospray tip (New Objective). Protein identification and characterization were performed by using the 4800 MALDI TOF/TOF Analyser (ABSciex) which was equipped with a Nd:YAG laser that operates at 355 nm to ionize the samples. All mass spectra were acquired in positive ion reflector mode using the 4000 series explorer version 3.5.28193 software (ABSciex). Each sample was analyzed with MALDI-TOF MS to create the peptide mass fingerprinting (PMF) data (scanning range of 900-4000 m/z). The peak detection criteria for MS/MS used were an S/N of 5 and a local noise window width of 250 (m/z) and a minimum full-width half maximum (bins) of 2.9. The combined PMF and MS/MS search was then performed using GPS Explorer algorithm version 3.6 (ABSciex) against the non-redundant NCBInr database using the in-house MASCOT search engine version 2.2. The criteria for protein identification were based on the probability score of each search result. Significant matches had scores greater than the minimum threshold set by MASCOT ($P < 0.05$).

DNA manipulation and plasmid construction

The strains, plasmids and primers used for protein overexpression are listed in Table S3 and S4. The *E. coli* XL1-Blue and BL21 (DE3) strains harboring designated vectors were cultured in LB medium supplemented with 0.1 mg/ml ampicillin. All the plasmids used as templates for PCR were extracted by using the plasmid extraction kit (QIAprep Spin Miniprep kit, QIAGEN). All PCR primers were synthesized by BGI Company (Guangdong, China). The *gapdh and idh* genes were amplified by PCR using *E. coli* MG1655 chromosomal DNA as a template and the primers are listed in Table S4, which contains AgeI and EcoRI restriction sites at the 5'- and 3'-end respectively. The corresponding amplified products were digested with AgeI and EcoRI and ligated into the pHisSUMO plasmid,[3] which has been digested with the same restriction enzymes. The generated plasmid pHisSUMO-*gapdh* and pHisSUMO-*idh* was extracted and transformed into BL21 (DE3) cells for protein expression.

Protein expression and purification

Overnight cultures of BL21 (DE3) cells harboring the pHisSUMO-*gapdh* plasmid were diluted by 1:100 to fresh LB medium supplemented with 100 µg/ml ampicillin. Cells were grown at 37 °C with rotations of 200 rpm until the OD_{600} reached 0.6. GAPDH and IDH expression was induced by addition of 200 µM isopropyl-β-D-thiogalactoside (IPTG) and the bacteria were further cultured for 16 hours at 25 °C. The bacteria were harvested by centrifugation (5000 g, 20 minutes at 4 °C) and the cell pellets were resuspended with 35 mM Tris-HNO_3 (pH=7.4), 100 mM $NaNO_3$ buffer and lysed by sonication. The lysates were centrifuged at 15000 g for 30 mins, and the supernatant was collected and then applied to a 5 ml HisTrap Q column (GE Healthcare). The proteins were eluted with 300 mM imidazole in 35 mM Tris-HNO_3 buffer (pH=7.4) with 100 mM $NaNO_3$. The eluted proteins were further subjected to SUMO protease cleavage (50 NIH units) at 25 °C for 2 hours to remove the His-

tag. They were further purified by a HiLoad 16/60 Superdex 200 column equilibrated with Tris-HNO_3 buffer (35 mM Tris-HNO_3 buffer (pH=7.4) and 100 mM $NaNO_3$. The identity of the purified GAPDH and IDH was further confirmed by MALDI-TOF MS. Plasmids for $GAPDH^{C149S}$, $GAPDH^{C153S}$, $GAPDH^{H176S}$, $GAPDH^{C288S}$, $GAPDH^{C149S/H176S}$, and $GAPDH^{3CS}$ mutants were generated *via* site-directed mutagenesis using Phusion high fidelity DNA polymerase (NEB). The wild-type pHisSUMO-*gapdh* plasmid was used as the DNA template and the success of the site-directed mutations were verified by DNA sequencing (BGI). The primers used for the mutants are listed in Table S4. The expression and purification of GAPDH mutants were identical to wild-type GAPDH.

GE-ICP-MS of purified proteins

Typical one dimensional GE-ICP-MS[2] was employed to measure the silver-binding capability of purified proteins GAPDH and IDH. The concentration and length of freshly prepared column gel was optimized and all the purified proteins were subjected to the same separation conditions. In detail, 2.5 cm of 12% resolving gel and 0.6 cm 4% stacking gel were used. For the GE-ICP-MS test, 10 µl of 4 µM protein samples were injected. ^{127}I-labelled proteins were used as internal standards to calibrate the MWs and intensities of Ag^+-binding proteins.

Cellular thermal shift assay (CETSA)

The cellular thermal shift assay was performed according to a standard method.[4] In brief, overnight cultures of wild type *E. coli MG1655* were diluted by 1:100 in an LB broth. Cells were cultured to an OD_{600} of 0.3 at 37 °C and further cultured for 1 hour in the absence or presence of 24 µM $AgNO_3$. The bacterial pellets were harvested and washed with PBS for 4 times. Equal amounts of the cell suspensions were aliquoted into PCR tubes and heated individually at increasing temperatures ranging from 50 °C to 80 °C for 3 minutes in a 96-well thermal cycler. The tubes were cooled immediately at room temperature for another 3 minutes after heating, and the heating procedures were repeated for 3 times. The cells were lysed by freeze-thaw cycles for five cycles in liquid nitrogen and thermal cycler set at 25 °C. The cell lysates were then centrifuged at 20, 000×g for 10 minutes at 4 °C to obtain the supernatant. The soluble proteins in the supernatants were subjected to gel electrophoresis and immune-blotting using GAPDH antibodies.

Protein oligomerization state analysis

The oligomerization states of GAPDH were analyzed by size-exclusion chromatography. GAPDH proteins were incubated with different molar equivalents of Ag^+ at room temperature for 1 hr. The elution volumes of the samples were subsequently measured on a Superdex 200 column (GE Healthcare), pre-equilibrated with a Tris-HNO_3 buffer (35 mM Tris-HNO_3 buffer, 100 mM $NaNO_3$, pH=7.4). The column was pre-calibrated with a GE LMW calibration kit.

***In vivo* enzymatic activity measurement**

Colorimetric assay kits of glyceraldehyde 3-phosphate dehydrogenase (Abcam) were used to measure the corresponding enzymatic activities. In brief, *E. coli* cell cultures after treatment with different concentrations of $AgNO_3$ were harvested, washed, resuspended and lysed in lysis buffers with sonication. The protein concentration of the supernatant after centrifugation was measured by a bicinchoninic acid assay (Pierce BCA Protein Assay Kit, Thermo Scientific). Enzyme activities

were measured according to the procedures provided by the manufacturers. The enzyme activity was normalized to protein concentration.

Mass spectrometry of purified proteins

The silver contents in GAPDH and its mutants were measured by Matrix Assisted Laser Ionization Time-of-Flight Mass Spectrometry (MALDI-TOF MS) (Bruker ultraflex extreme MALDI-TOF-TOF-MS). Wild-type GAPDH and $GAPDH^{3CS}$ were incubated with different molar equivalents of Ag^+ at room temperature for 1 hour. Saturated sinapic acid in 1:1 ACN:H_2O was prepared as the matrix. In detail, 1 µl of proteins with a concentration of 10 µM in water was mixed with 1 µl of matrix, *i.e.*, saturated sinapic acid in 50:50 ACN:H_2O, and crystalized on polished 384 well plate prior to MALDI-TOF MS analysis. Mass spectra were measured in the positive linear mode.

Silver content determination in GAPDH and mutant proteins

The silver contents of proteins were determined by ICP-MS. All ICP-MS experiments were conducted on the Agilent 7700x system. 4 molar equivalents of Ag^+ were added into approximate 200 µM GAPDH, $GAPDH^{C149S}$, $GAPDH^{C153S}$, $GAPDH^{H176S}$, $GAPDH^{C288S}$ and $GAPDH^{3CS}$ in Tris-HNO_3 buffer. After incubation for 1 hour at room temperature, excess amounts of Ag^+ were removed by a HiTrap desalting column (GE healthcare). The eluted protein concentration was measured by a bicinchoninic acid (BCA) assay. The standard curve of silver was prepared from a multielement standard solution (90243, Sigma-Aldrich) for ICP-MS. Silver contents in proteins were calculated according to the standard curve.

Ellman assay

Different molar equivalents of Ag^+ were added into 80 µM GAPDH or mutants and incubated for 30 minutes at room temperature. Excess amounts of 5, 5-dithio-bis-(2-nitrobenzoic acid) (DTNB) were added with a final concentration of 300 µM. After further incubation for 20 minutes, UV absorbance for each sample at 412 nm was measured on a Cary 50 UV-vis spectrometer. The absorbance at 412 nm was plotted against the Ag^+/protein ratio. The Ellman assay was carried out in Tris-HNO_3 buffer (35 mM Tris-HNO_3 buffer, 100 mM $NaNO_3$, pH=7.4).

Isothermal titration calorimetry

The GAPDH, $GAPDH^{C149S}$, $GAPDH^{C153S}$, $GAPDH^{C288S}$ and $GAPDH^{3CS}$ were prepared in a Tris-HNO_3 buffer (35 mM Tris-HNO_3 buffer, 100 mM $NaNO_3$, pH=7.4) with a final concentration of 20 µM. About 600 µM $AgNO_3$ dissolved in Tris-HNO_3 buffer were prepared as a titrant. Generally, 40 µl of $AgNO_3$ were titrated into 200 µl protein samples with 90 second intervals between each injection. The signals of the titration of $AgNO_3$ with the Tris-HNO_3 buffer were recorded as the background. All isothermal titration calorimetry (ITC) experiments were performed on a Malvern MicroCal ITC200 at 25 ^oC and all data were analyzed using the Origin software and fitted by one-set-of-site binding models.

Enzyme inhibition assay

Freshly prepared 16 µM of GAPDH, $GAPDH^{C149S}$, $GAPDH^{C153S}$, $GAPDH^{H176S}$, $GAPDH^{C288S}$ and $GAPDH^{3CS}$ in a Tris-HNO_3 buffer (35 mM Tris-HNO_3 buffer, 100 mM $NaNO_3$, pH=7.4) were incubated with various concentrations of Ag^+ for 1 hour at room temperature. The protein mixtures were further diluted to 600 nM and the enzyme activities were measured with the

Glyceraldehyde-3-phosphate dehydrogenase (GAPDH) assay kit (Abcam). The absorbance at 450 nm was monitored constantly for a duration of 20 minutes. The initial rates were calculated from each reaction curves to fit the IC_{50} curves.

Michaelis-Menten kinetics

Freshly prepared 16 μM of GAPDH proteins were incubated with 0, 1, 2 and 3 equivalents of Ag^+ for 1 hour at room temperature. The enzymatic activity was measured with glyceraldehyde 3-phosphate (G3P) as the substrate, ranging from 0.25 to 16 mM. The K_M and V_{max} for both the uninhibited and inhibited reactions were obtained by fitting the data into the double reciprocal Lineweaver-Burk plots. The apparent K_i values were calculated by using a mixed-type inhibition model with the following equations (equation 1 and 2).

$$V_{max}\text{App} = V_{max}\,(1+\frac{[\text{Ag}^+]}{K_i'}) \qquad \text{Equation 1}$$

$$K_M\text{App} = K_M\,\frac{(1+\frac{[\text{Ag}^+]}{K_i})}{(1+\frac{[\text{Ag}^+]}{K_i'})} \qquad \text{Equation 2}$$

V_{max}App, apparent V_{max}; K_MApp, apparent K_M.

X-ray crystallography

Crystals of wild-type apo-GAPDH were grown using the hanging-drop vapor diffusion method. The precipitant contains 0.15 M D, L-malic acid and 20% PEG 3350 (w/v). Octahedral crystals appeared within three days and grew up to full size within one week. Silver-bound GAPDH was prepared by incubating the apo-GAPDH protein with 4 eq. of $AgNO_3$ for 1 hr and removing excess silver by a desalting column. Ag-GAPDH was crystalized under the same condition as the apo-GAPDH. For the soaking experiment, crystals of apo-GAPDH were soaked into a cryo-protectant solution (0.15 M D, L-malic acid, 20% PEG 3350 (w/v), 20% glycerol (v/v) and 2 mM $AgNO_3$) for various time periods before being cryo-cooled. The diffraction data were collected at the BL17U beamline of Shanghai Synchrotron Radiation Facility (SSRF), by using 0.97914 Å synchrotron radiation.[5] The diffraction data were processed with XDS [6]. The CCP4 suite [7] and Phenix [8] were used for data refinement and finalization. An apo-GAPDH structure was used as the model for molecular replacement [9]. TLS refinement was used in the later stage of data processing. The coordinates and structure factors for the apo-GAPDH, Ag-GAPDH-1, and Ag-GAPDH-2 were deposited at protein databank with accessing code 6IOJ, 6IO4, and 6IO6.

Effect of Ag^+ on *E. coli* growth

The minimum inhibitory concentration (MIC) values of Ag^+ against wild-type *E. coli* and *E. coli* GAPDH$^{C149S/H176S}$ mutants were measured using the standard two fold dilution method. Briefly, wild-type *E. coli* and *E. coli* GAPDH$^{C149S/H176S}$ were cultured in LB broth overnight at 37 °C. The bacterial density was adjusted to around 1×10^5 CFU/ml according to the measurement of optical density at 600 nm (OD_{600}) and CFU counting on agar plates. $AgNO_3$ was added into 96-well plates in triplicates and performed 2-fold serial dilution, followed by addition of bacterial inocula and further incubation at 37 °C overnight. Wells without addition of $AgNO_3$ were used as controls and wells with culture media only as background. The MIC_{50} was determined as the concentration that can inhibit 50% growth of the bacteria.

Statistical analysis

Unless specified, all experiments were subjected to three biological replicates and two technique replicates. A two-tailed t-test was used for all comparisons between two groups. Data are presented as mean ± SEM. *P < 0.05, **P < 0.01 and ***P < 0.001. NS, not significant (P > 0.05).

Supplementary Figures

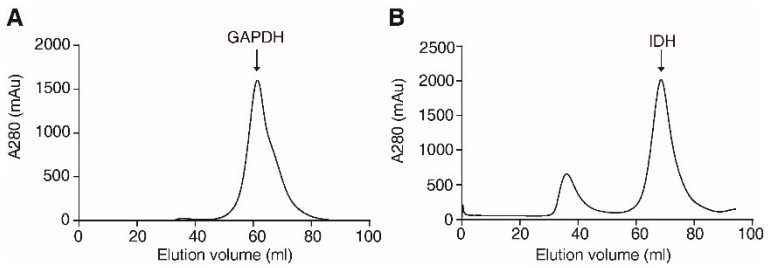

Figure S1. Overexpression and purification of GAPDH and IDH. Gel filtration profile of GAPDH (A) and IDH (B) on a column Hiload 16/60 Superdex 200 (GE Healthcare) pre-equilibrated with 35 mM Tris-HNO_3, 100 mM $NaNO_3$, pH=7.4.

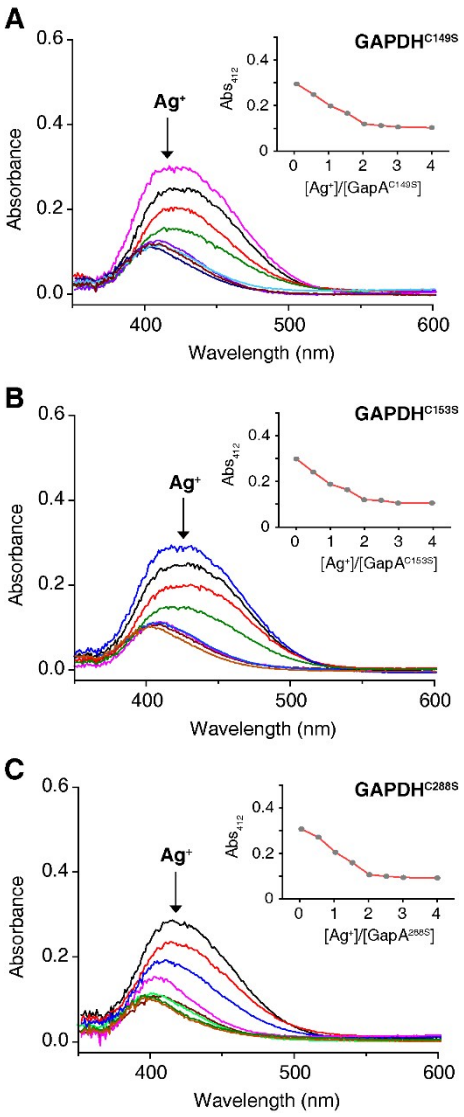

Figure S2. Ag^+ binding to GAPDH mutants monitored by Ellman's assay. (A) $GAPDH^{C149S}$. (B) $GAPDH^{C153S}$. (C) $GAPDH^{C288S}$. Proteins were pre-incubated with various molar equivalents of Ag^+ as indicated by the inserted plots. The free thiol contents in the protein samples were measured by adding excess amounts of DTNB (Ellman's reagent). The absorbance at 412 nm was plotted against Ag^+/protein ratios. One representative of three replicates is shown (A, B, C).

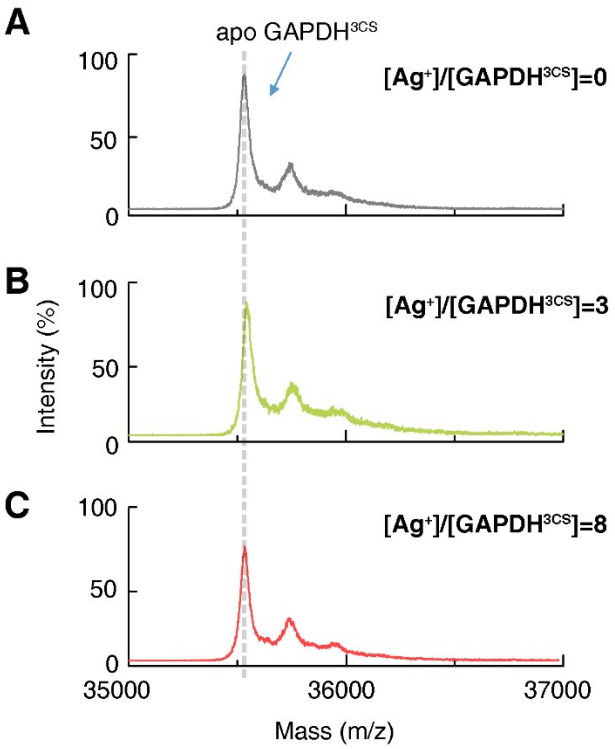

Figure S3. Mass spectra of GAPDH^{3CS} with or without incubation of Ag^+. (A) GAPDH^{3CS} without incubation with Ag^+. (B) GAPDH^{3CS} with incubation with 3 eq. of Ag^+. (C) GAPDH^{3CS} with incubation with 8 eq. of Ag^+.

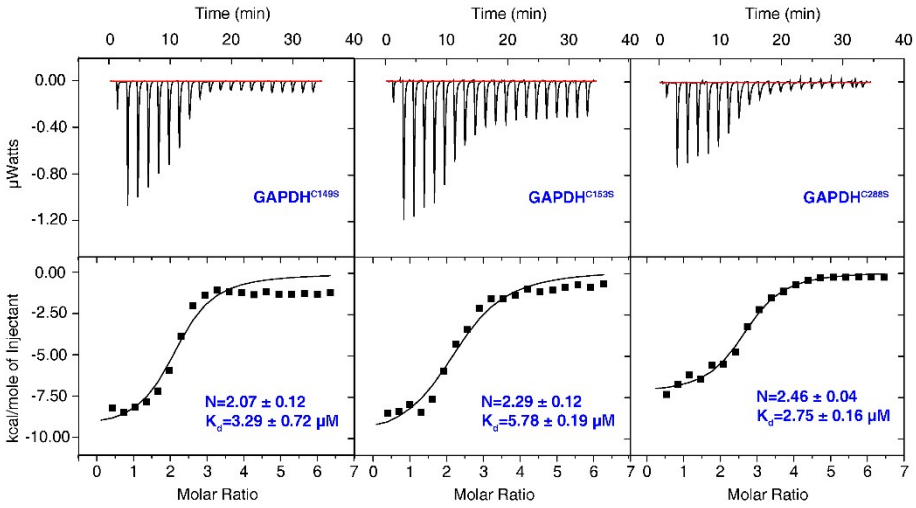

Figure S4. Isothermal titration calorimetry (ITC) results of Ag^+ binding to GAPDH mutants $GAPDH^{C149S}$, $GAPDH^{C153S}$ and $GAPDH^{C288S}$ (n=3). The titrations were carried out at 25 °C in 35 mM Tris-HNO_3 and 100 mM $NaNO_3$ buffer at pH 7.4. The data were fitted to a one-set-of-site binding model using the Origin software. Mass spectra of $GAPDH^{3CS}$ with or without incubation of Ag^+. One representative of three replicates is shown. The results are shown as mean ± SEM.

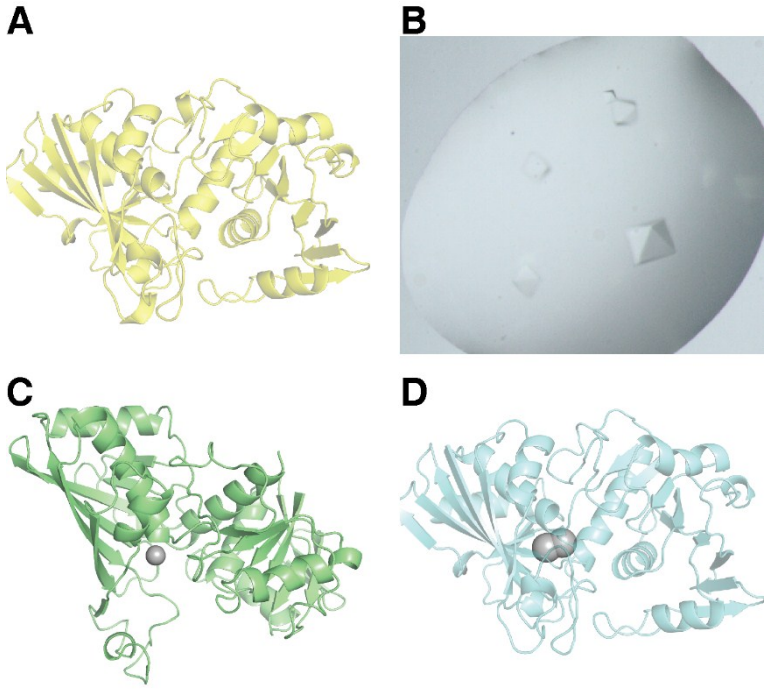

Figure S5. Crystal and structure of apo and Ag-bound GAPDH. (A) The overall structure of apo GAPDH in cartoon representation. (B) The picture of Ag-GAPDH-1 crystal. Overall structure of Ag-GAPDH-1 with silver binding at Cys149/His176 site (C) and Ag-GAPDH-2 with silver binding at Cys288 site (D) (Ag^+ in grey sphere).

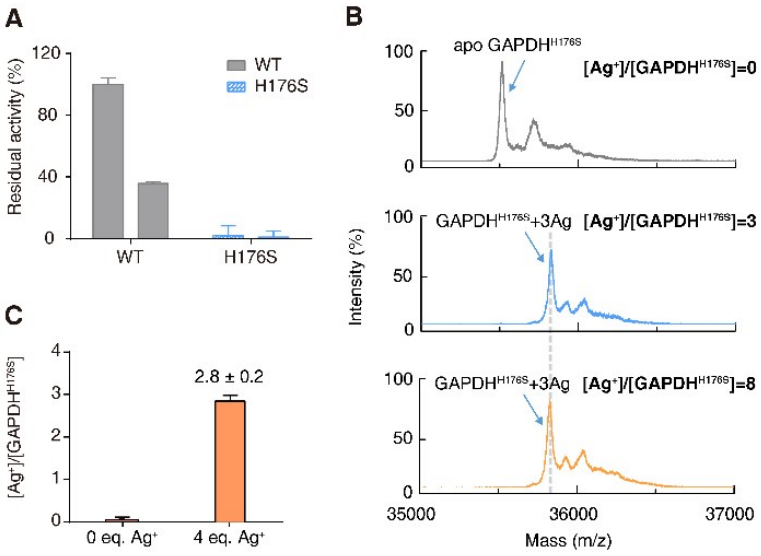

Figure S6. The effect of site-directed mutation of His176 to Ser on the function of GAPDH. (A) Normalized residual activity of WT GAPDH and GAPDH^{H176S} in the absence (left) and presence of 3 eq. of Ag^+ (right) (n=3). (B) MALDI-TOF MS of apo-GAPDH^{H176S} and GAPDH^{H176S} after incubation with 2 eq. and 8 eq. of Ag^+. (C) Stoichiometry of Ag^+ binding to GAPDH^{H176S} measured by ICP-MS (n=3). The results are shown as mean ± SEM (A, C).

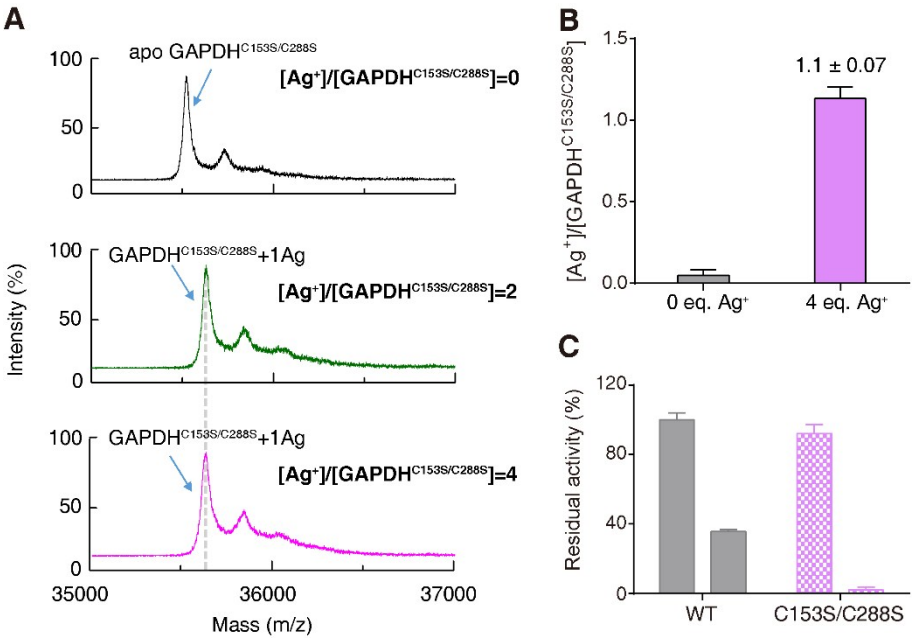

Figure S7. The effect of site-directed mutation of Cys153 and Cys288 to Ser on the function of GAPDH. (A) MALDI-TOF MS of apo-GAPDH$^{C153S/C288S}$ and GAPDH$^{C153S/C288S}$ after incubation with 2 eq. and 4 eq. of Ag^+. (B) Stoichiometry of Ag^+ binding to GAPDH$^{C153S/C288S}$ measured by ICP-MS (n=3). (C) Normalized residual activity of WT GAPDH and GAPDH$^{C153S/C288S}$ in the absence (left) and presence of 2 eq. of Ag^+ (right) (n=3). The results are shown as mean ± SEM (B, C).

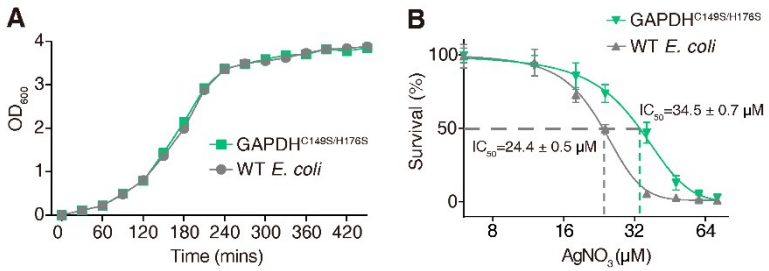

Figure S8. Bacterial growth and IC_{50} test. (A) Bacterial growth curves of wild-type *E. coli* and GAPDH$^{C149S/H176S}$ variant. The OD_{600} was recorded at 30 min intervals (n=3). (B) Measurement of IC_{50} values of Ag^{+} against *E. coli* and wild-type *E. coli* and GAPDH$^{C149S/H176S}$ variant (n=3). The experiment was performed in a 96-well plate and the OD_{600} of each well was measured. The Ag^{+} inhibition curves were plotted. All experiments were performed in triplicates. One representative of three replicates is shown (A). The results are shown as mean ± SEM (B).

Supplementary Tables

Table S1. Summary of standard proteins used for iodine labelling in this study.

	Theoretical		**Calibrated**	
Full name	Symbol	MW/kDa	Symbol	MW/kDa
Ribonuclease A	RA	13.7	I-RA	15.5
Carbonic anhydrase	CA	30.0	I-CA	31.0
Ovalbumin	OVA	44.0	I-OVA	45.3
Conalbumin	OTF	75.0	I-OTF	76.0

Table S2. Summary of identified Ag^+-binding proteins in *E. coli*.

Gene	Gene product	MW/ kDa	Accession No.	Protein Score	Protein Score C.I.%	Peptide count
ZraP	Zinc resistance-associated protein	15.2	gi|545173305	110	100	5
SodA	Superoxide dismutase [Mn]	23.1	gi|486185058	130	100	6
SucD	Succinyl-CoA synthetase subunit alpha	30.0	gi|693092162	214	100	9
GAPDH	Glyceraldehyde-3-phosphate dehydrogenase	35.7	gi|693197584	330	100	14
IDH	Isocitrate dehydrogenase	46.1	gi|754720090	165	100	13
AceB	Malate synthase A	60.6	gi|545255278	540	100	15

Table S3. Strains, plasmids for protein expression.

Strains	**Application**
XL1-Blue	Plasmid maintenance
BL21(DE_3)	Protein expression
Plasmids	
pHisSUMO	
pHisSUMO-*gapdh*	Wide-type GAPDH protein expression
pHisSUMO-*gapdh* ^{C149S}	GAPDH^{C149S} mutant protein expression
pHisSUMO-*gapdh*^{C153S}	GAPDH^{C153S} mutant protein expression
pHisSUMO-*gapdh* ^{C288S}	GAPDH^{C288S} mutant protein expression
pHisSUMO-*gapdh* ^{H176S}	GAPDH^{H176S} mutant protein expression
pHisSUMO-*gapdh*^{3CS}	GAPDH^{3CS} mutant protein expression
pHisSUMO-*zrap*	Wide-type Zrap protein expression
pHisSUMO-*idh*	Wide-type IDH protein expression

Table S4. Primers for plasmid construction.

	Forward Primers (AgeI)	Reverse Primers (EcoRI)
GAPDH	ATTCACCGGTGGAATGACTATCAAAGTAGG	CCGGAATTCTTATTTGGAGATGTGAGCG
$GAPDH^{C149S}$	GCTTCCAGCACCACCAAC	GTTGGAAACGATGTCCTG
$GAPDH^{C153S}$	CACCAACAGCCTGGCTCC	GTGCAGGAAGCGTTGGAA
$GAPDH^{H176S}$	ACCGTTAGCGCTACTAC	GGTCATCAGACCTTCG
$GAPDH^{C288S}$	CGAAGTTAGCACTTCCGTG	CCGTTGAAATCGGTAGA
IDH	ATTCACCGGTGGAATGGAAAGTAAAGTAG	CCGGAATTCTTACATGTTTTCGATG
ZraP	ATTCACCGGTGGAATGAAACGGAACAC	CCGGAATTCTTACCAGTGGCC

Table S5. Summary of isothermal titration calorimetry data.

Protein	Ligand	N	*K*d (μM)	ΔH (kcal mol^{-1})	ΔS (cal mol^{-1} K^{-1})
GAPDH	Ag^{+}	N = 3.38 ± 0.04	*K*d = 0.90 ± 0.04	ΔH= -10.21 ± 0.19	ΔS = -6.59
$GAPDH^{C149S}$	Ag^{+}	N = 2.07 ± 0.12	*K*d = 3.29 ± 0.72	ΔH = -10.24 ± 0.82	ΔS = -9.27
$GAPDH^{C153S}$	Ag^{+}	N = 2.29 ± 0.12	*K*d = 5.78 ± 0.19	ΔH = -12.2 ± 0.80	ΔS = -16.9
$GAPDH^{C288S}$	Ag^{+}	N = 2.46 ± 0.04	*K*d = 2.75 ± 0.16	ΔH = -8.03 ± 0.20	ΔS = -1.48
$GAPDH^{3CS}$	Ag^{+}	Not detectable			

Table S6. Enzyme kinetics of GAPDH with or without treatment of Ag^+.

$[Ag^+]$/[GAPDH]	0	1	2	3
V_{max} (μmol/min/mg)	3.3 ± 0.23	2.5 ± 0.15	1.7 ± 0.17	0.50 ± 0.04
K_M (mM)	1.15 ± 0.28	1.22 ± 0.26	8.39 ± 0.98	9.24 ± 1.29

Table S7. Summary of X-ray crystallographic data collection and refinement statistics.

	Ag-GAPDH-1[a]	Ag-GAPDH-2[b]	apo-GAPDH
Wavelength (Å)	0.97914	0.97914	0.97914
Resolution range (Å)	84.70 - 3.10 (3.21 - 3.10)	48.32 – 2.64 (2.74 - 2.64)	39.02 – 2.29 (2.37 – 2.29)
Space group	*P*1	$I4_122$	$I4_122$
a, b, c (Å)	87.99, 110.02, 139.71	122.26, 122.26, 157.78	120.89, 120.89, 156.07
α, β, γ (°)	87.66, 86.94, 87.26	90.00, 90.00, 90.00	90.00, 90.00, 90.00
Unique reflections	85568 (8834)	17911 (1758)	26218 (2611)
Completeness (%)	90.24 (92.86)	99.74 (99.21)	99.45 (99.73)
Mean I/sigma(I)	8.50 (2.10)	8.40 (2.03)	18.30 (2.79)
Wilson B-factor	81.25	74.31	54.91
R-merge	0.0809 (0.468)	0.143 (0.399)	0.117 (0.287)
R-meas	0.115 (0.662)	0.202 (0.565)	0.165 (0.406)
R-pim	0.0550 (0.331)	0.143 (0.399)	0.117 (0.287)
Reflections for refinement	85568 (8834)	17889 (1751)	26200 (2610)
R-work	0.190 (0.299)	0.193 (0.349)	0.189 (0.273)
R-free	0.241 (0.356)	0.236 (0.382)	0.222 (0.341)
Number of non-hydrogen atoms	39562	2487	2519
RMSD (bonds) (Å)	0.001	0.006	0.006
RMSD (angles) (°)	0.41	0.84	0.79
Ramachandran favored (%)	93.81	94.50	95.11
Ramachandran allowed (%)	5.71	5.20	4.59
Ramachandran outliers (%)	0.48	0.31	0.31
Rotamer outliers (%)	0.00	0.00	0.76
Clashscore	4.52	5.20	6.25
Average B-factor	98.39	84.41	70.30
Number of TLS groups	126	8	2

*Statistics for the highest-resolution shell are shown in parentheses.

[a] Crystal of directly crystalized Ag-bound GAPDH.

[b] GAPDH crystal soaked with 2 mM Ag^{+} for 10 min.

References

[1] N. Jakubowski, J. Messerschmidt, M. G. Anorbe, L. Waentig, H. Hayen, P. H. Roos, *J. Anal. At. Spectrom.* 2008, *23*, 1487-1496.

[2] L. Hu, T. Cheng, B. He, L. Li, Y. Wang, Y.-T. Lai, G. Jiang, H. Sun, *Angew. Chem. Int. Ed.* 2013, *52*, 4916-4920.

[3] Y. H. Fong, H. C. Wong, M. H. Yuen, P. H. Lau, Y. W. Chen, K. B. Wong, *PLoS Biol.* 2013, *11*, e1001678.

[4] R. Jafari, H. Almqvist, H. Axelsson, M. Ignatushchenko, T. Lundback, P. Nordlund, D. Martinez Molina, *Nat. Protoc.* 2014, *9*, 2100-2122.

[5] Q.-S. Wang, K.-H. Zhang, Y. Cui, Z.-J. Wang, Q.-Y. Pan, K. Liu, B. Sun, H. Zhou, M.-J. Li, Q. Xu, C.-Y. Xu, F. Yu, J.-H. He, *Nucl. Sci. Tech.* 2018, *29*, 68.

[6] W. Kabsch, *Acta Crystallogr. D* 2010, *66*, 125-132.

[7] Collaborative, *Acta Crystallogr. D* 1994, *50*, 760-763.

[8] P. D. Adams, P. V. Afonine, G. Bunkoczi, V. B. Chen, I. W. Davis, N. Echols, J. J. Headd, L.-W. Hung, G. J. Kapral, R. W. Grosse-Kunstleve, A. J. McCoy, N. W. Moriarty, R. Oeffner, R. J. Read, D. C. Richardson, J. S. Richardson, T. C. Terwilliger, P. H. Zwart, *Acta Crystallogr. D* 2010, *66*, 213-221.

[9] A. J. McCoy, R. W. Grosse-Kunstleve, P. D. Adams, M. D. Winn, L. C. Storoni, R. J. Read, *J. Appl. Crystallogr.* 2007, *40*, 658-674.